Importance of nucleon-nucleon interactions in hardening nucleon spectra in heavy ion fusion

E. Fabrici, E. Gadioli, E. Gadioli Erba, and M. Galmarini
Dipartimento di Fisica, Università di Milano, Istituto Nazionale di Fisica Nucleare, Sezione di Milano, Milano, Italy

F. Fabbri and G. Reffo
Ente Nazionale Energie Alternative, Divisione di Calcolo, 40138 Bologna, Italy
(Received 26 June 1989)

The thermalization of the composite system created in the fusion of two heavy ions at an incident energy of 20–30 MeV/nucleon and the emission of fast nucleons before the attainment of statistical equilibrium are described by means of the Harp-Miller-Berne master equation approach. The incident energy is transformed into excitation energy by two-body nucleon-nucleon interactions, assuming that the mean field readjusts itself instantaneously as the two ions fuse. Symmetric and asymmetric systems have been investigated. The results indicate the paramount importance, in the case of symmetric systems, of interactions between high-energy nucleons, one of which scatters to a deep-hole state, thus producing the higher-energy particles observed experimentally.

I. INTRODUCTION

At very low relative energies the time evolution of the dinuclear system created as two heavy ions stick together is described by the time-dependent Hartree-Fock (TDHF) theory[1,2] and two-body collisions are thought to be of minor importance, being hindered by the Pauli principle. As the relative energy of the two heavy ions increases, the Pauli blocking becomes less effective and intranucleon collisions can no longer be neglected.

A way to take into account both effects, mean-field and nucleon-nucleon collisions, is based on a semiclassical approximation that leads to the Vlasov-Uehling-Uhlenbeck (VUU) equation[3,4] for a nucleon phase space distribution function $f(\mathbf{r},\mathbf{p},t)$, whose evolution in time is determined by the mean-field dynamics and by intranuclear collisions. A method to improve these calculations, of semiclassical nature, while retaining their physical assumptions, has been indicated by Cassing.[5–7] Cassing separates in time the action of the mean-field and of nucleon-nucleon interactions. The mean-field interaction is dominant before the two nuclei come in contact, and the subsequent time evolution is ruled by nucleon-nucleon interactions. The mean-field interaction is evaluated by TDHF theory and provides an average momentum space distribution $f_{\mathrm{av}}(\mathbf{k},t=0)$ for nucleons in the dinuclear interaction region, whose subsequent time evolution depends on the nucleon-nucleon interactions and emissions to the continuum. These two approaches take into account, to a different degree of accuracy, the so-called one-body dissipation mechanism, due to the mean-field acting on the interacting ions, and the two-body dissipation mechanism occurring *via* two-body nucleon-nucleon interactions.

A number of calculations of nucleon spectra has also appeared in literature considering explicitly only the two-body interaction mechanism,[8,9] and these are more directly related to the calculations of preequilibrium cross sections made in the case of light projectiles.

To reproduce the spectral distribution of the emitted nucleons one has to consider only the momentum distribution of the nucleons in the target and the projectile, the information on the configuration space being unnecessary.[5–7,8] In the Thomas-Fermi approximation, the density of states of the nucleons bound in a potential well does not change appreciably for not too large variations of the $\mathbf{r}$ dependence of the mean field, in the case of incompressible nuclear matter and volume-conserving deformations.[10] If these conditions are approximately satisfied during the time evolution of the dinuclear system, its relaxation may be described by the Harp-Miller-Berne (HMB) master equation approach,[11,12] which allows one to evaluate the time evolution of the energy distribution of the nucleons, as resulting from two-body nucleon-nucleon interactions and from the emission of particles into the continuum. The HMB master equations correspond to the collision term in the VUU equation[3,4] and the Cassing theory,[7] but it differs from them in various respects, for instance in treating the emission of nucleons to the continuum, introducing, to describe this process, decay rates not explicitly considered in previous approaches.

The HMB master equations will be discussed in Sec. II of this paper together with a new proposal to evaluate the decay rates for nucleon-nucleon interactions, removing the approximation of orthogonal nucleon collision geometry used so far and taking into account linear momentum conservation in addition to energy conservation.

The outcome of the calculation depends in an essential way on the initial nucleon energy distribution $n_i(t=0)$ that will be evaluated, as discussed in Sec. III, by coupling the internal momentum of the projectile and the target nucleons with the translational momentum of the colliding ions with respect to their common center of mass, as done by Bondorf *et al.*[13] and Robel and Swiatecki[14] in the promptly emitted particles (PEP) and Fermi jet calculations. This procedure is essentially

based on the hypothesis that the asymptotic momentum distribution of the colliding nucleons is not greatly changed by the mean-field interaction. This is found to be approximately true for reaction times smaller than ≈ 30 fm$/c = 10^{-22}$ sec, when mean-field interactions dominate, both in the case of VUU and TDHF theory.[4,5,7] However, at larger interaction times, TDHF calculations show that a considerable distortion of the momentum distribution may occur with a reduction of low-momentum components and an enhancement of high-momentum components. It has been suggested that this may be of greater importance to reproduce the hardest part of the experimental nucleon spectra.[5-7] An analogous effect has been found also in VUU calculations.[15] This argument will be considered later; here it may be sufficient to remark that the use of the HMB master equations is not bound to the use of the initial distribution we use here.

The distribution $n_i(t=0)$, evaluated as already briefly indicated, is characterized by holes, in addition to excited particles, whose number and excitation energy depends on the projectile-target mass symmetry and on the incident energy. The presence of these holes allows, as the intranucleon cascade develops, the excitation of particles to an energy higher than that resulting from the coupling of the internal and translational momenta. One of the main aims of this work is to investigate quantitatively the importance of this effect.

In Sec. IV we compare the theoretical predictions with the experimental data concerning nucleon emission in fusion and quasifusion processes of both symmetric and asymmetric systems at incident energies between 20 and 30 MeV/nucleon. Sec. V will be devoted to the conclusions.

II. HMB MASTER EQUATIONS

In this theory the nucleon states are classified according to their energy, ϵ, and divided into bins of width $\Delta\epsilon$. The number N_i of occupied states within each bin is equal to the product of the total number of states for that bin, g_i, times an occupation number $0 \le n_i \le 1$. Nucleons in states within bins i and j may interact and scatter to states within bins l and m subject to the conservation of energy and the availability of unoccupied states in l and m. Unbound nucleons may also escape from the nucleus with energy $\epsilon_i' = \epsilon_i - \epsilon_F - B_i$ (ϵ_F and B_i are, respectively, the Fermi energy and the binding energy of the nucleon in the composite nucleus) thus contributing to precompound emission. The relaxation of the nucleus, described as a two-fermion gas, is described by the master equations (written, in the following, for the proton gas, those for the neutron gas being the same with obvious substitutions):

$$\begin{aligned}\frac{d(n_i g_i)^\pi}{dt} = &\sum_{jlm}\left[\omega^{\pi\pi}_{lm\to ij} g_l^\pi n_l^\pi g_m^\pi n_m^\pi (1-n_i^\pi)(1-n_j^\pi)\left[\frac{g_i^\pi g_j^\pi}{\Delta\epsilon}\right]\delta(\epsilon_i^\pi+\epsilon_j^\pi-\epsilon_l^\pi-\epsilon_m^\pi)\right.\\ &\left.-\omega^{\pi\pi}_{ij\to lm} g_i^\pi n_i^\pi g_j^\pi n_j^\pi (1-n_l^\pi)(1-n_m^\pi)\left[\frac{g_l^\pi g_m^\pi}{\Delta\epsilon}\right]\delta(\epsilon_i^\pi+\epsilon_j^\pi-\epsilon_l^\pi-\epsilon_m^\pi)\right]\\ &+\sum_{jlm}\left[\omega^{\pi\nu}_{lm\to ij} g_l^\pi n_l^\pi g_m^\nu n_m^\nu (1-n_i^\pi)(1-n_j^\nu)\left[\frac{g_i^\pi g_j^\nu}{\Delta\epsilon}\right]\delta(\epsilon_i^\pi+\epsilon_j^\nu-\epsilon_l^\pi-\epsilon_m^\nu)\right.\\ &\left.-\omega^{\pi\nu}_{ij\to lm} g_i^\pi n_i^\pi g_j^\nu n_j^\nu (1-n_l^\pi)(1-n_m^\nu)\left[\frac{g_l^\pi g_m^\nu}{\Delta\epsilon}\right]\delta(\epsilon_i^\pi+\epsilon_j^\nu-\epsilon_l^\pi-\epsilon_m^\nu)\right]\\ &-n_i^\pi g_i^\pi \omega^\pi_{i-i'} g_{i'}^\pi \delta(\epsilon_i^\pi-\epsilon_F^\pi-B_i^\pi-\epsilon_{i'}^\pi)\ ,\end{aligned} \tag{1}$$

where π and ν stand, respectively, for the proton and the neutron.

The emission of particles to the continuum can be obtained by integrating the equations

$$\frac{dN_i'^\pi}{dt} = n_i^\pi g_i^\pi \omega^\pi_{i\to i'} g_{i'}^\pi \delta(\epsilon_i^\pi-\epsilon_F^\pi-B_i^\pi-\epsilon_{i'}^\pi)\ . \tag{2}$$

The total number of states within a given energy bin is evaluated in the framework of Fermi gas model and is given by

$$\begin{aligned} g_i &= \int_{\epsilon_i-\Delta\epsilon/2}^{\epsilon_i+\Delta\epsilon/2}\rho^\pi(\epsilon)d\epsilon\\ &= \frac{Z}{\epsilon_F^{3/2}}\left[\left[\epsilon_i+\frac{\Delta\epsilon}{2}\right]^{3/2}-\left[\epsilon_i-\frac{\Delta\epsilon}{2}\right]^{3/2}\right]\ .\end{aligned} \tag{3}$$

The decay rates for nucleon-nucleon interactions, $\omega_{ij\to lm} g_l g_m / \Delta\epsilon$, give the probability per unit time that two particles in a given state of the ith and the jth bin interact and scatter to the lth and the mth bin.

Assuming equiprobable all energy partitions between final particles, HMB gave for $\omega_{ij\to lm}$ the expression

$$\omega^{NN}_{ij\to lm} = \frac{\sigma_{NN} v_{ij}}{V\sum_{mn}(g_m^N g_n^N/\Delta\epsilon)\delta(\epsilon_i+\epsilon_j-\epsilon_m-\epsilon_n)}\ , \tag{4}$$

where V is the nuclear volume. The relative velocity v_{ij} was set equal to

$$v_{ij} = \left[\frac{2(\epsilon_i^N+\epsilon_j^N)}{M}\right]^{1/2} \tag{5}$$

(where M is the nucleon mass) assuming perpendicular directions of colliding particles, the most likely occurrence in case of nucleon-nucleon cross-section in-

dependent of the relative energy.

The decay rates for emission of particles into the continuum are

$$\omega_{i\to i'}=\frac{\sigma_{\rm inv}v_{i'}}{g_i\Omega}\ , \tag{6}$$

where $\sigma_{\rm inv}$, $v_{i'}$ and Ω are, respectively, the inverse cross section, the emitted nucleon velocity and the lab volume which cancels a similar factor appearing in the expression for $g_{i'}$.

Two of the approximations made in evaluating the decay rates for nucleon-nucleon interaction may be easily eliminated, namely, that of considering only perpendicular collision geometry, which is inconsistent with the assumptions of energy-dependent nucleon-nucleon cross sections, and that of considering as equiprobable any partition of initial energy between the final particles provided that their total energy is conserved. In fact linear momentum conservation leads to further restrictions on the possible values of the energies of the particles after scattering. In the following, the momentum of the nucleons is explicitly taken into account, and the corresponding energy is evaluated using the classical momentum-energy relation.

Once the linear momenta $\mathbf{p}_i$ and $\mathbf{p}_j$ of the colliding particles, in the projectile-target center-of-mass system, are given, the end points of the vectors representing the final momenta in the same system, $\mathbf{p}_l$ and $\mathbf{p}_m$, must be located on the surface of a sphere of diameter equal to the relative momentum of the two nucleons

$$2p=(p_i^2+p_j^2-2p_ip_j\cos\theta_{ij})^{1/2} \tag{7}$$

centered around their center of mass o, as shown in Fig. 1. Then, for any given pair of colliding nucleon momenta $\mathbf{p}_i$ and $\mathbf{p}_j$ any possible final momentum p_l must satisfy

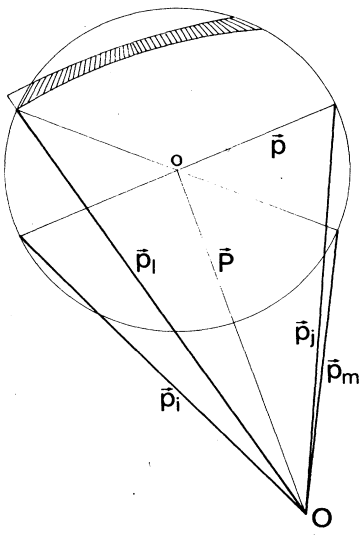

FIG. 1. In this figure is shown the sphere in momentum space, whose surface represents the locus where are confined the end points of vectors $\mathbf{p}_l$ and $\mathbf{p}_m$ once $\mathbf{p}_i$ and $\mathbf{p}_j$ are given.

the condition

$$|P-p|\le p_l\le P+p\ , \tag{8}$$

where $2\mathbf{P}=\mathbf{p}_i+\mathbf{p}_j$ and $p_i^2+p_j^2=p_l^2+p_m^2$.

Assuming an isotropic angular distribution of scattered particles in the two-nucleon center-of-mass system, the probability, $\Pi_{ij\to lm}$, of getting final momenta in the intervals Δp_l and Δp_m around the values p_l and p_m, starting from a pair $\mathbf{p}_i$ and $\mathbf{p}_j$, is equal to the ratio of the area of the shaded annulus in Fig. 1 (given by the intersection of the sphere of radius p, centered around the two-nucleon center of mass, o, and the two spheres of radii p_l and $p_l+\Delta p_l$, centered on the projectile-target center of mass, O) to the area of the sphere of radius p. Thus,

$$\Pi_{\rm ij\to lm}=\frac{p_l\Delta p_l}{2pP}=\frac{M\Delta\epsilon_l}{2pP} \tag{9}$$

when inequality (8) is satisfied, and zero otherwise. The decay rate for nucleon-nucleon interaction is

$$\omega^*_{\rm ij\to lm}=\frac{\sigma_{\rm ij}v_{\rm ij}\Pi_{\rm ij\to lm}}{V}\ , \tag{10}$$

where $\sigma_{\rm ij}$ and $v_{\rm ij}$ are the two-nucleon interaction cross section and relative velocity.

An often-encountered assumption in such calculations consists in using proton-proton (neutron-neutron) and proton-neutron cross sections, $\sigma_{\rm ij}^{\pi,\pi(\nu\nu)}$ and $\sigma_{\rm ij}^{\pi\nu}$, that vary with the inverse of the energy with a constant ratio r, between them:[16]

$$\sigma_{\rm ij}^{\pi\pi(\nu\nu)}=\frac{K}{E_{\rm ij}}\left[\frac{r}{r+1}\right] \tag{11a}$$

and

$$\sigma_{\rm ij}^{\pi\nu}=\frac{K}{E_{\rm ij}}\left[\frac{1}{r+1}\right]\ , \tag{11b}$$

where $E_{\rm ij}$ is the two-nucleon relative energy. In the case of free nucleon-nucleon cross sections, $K\approx 500$ fm^2 MeV, while, when only the residual interaction is effective, as it should be within the nucleus, its value might be substantially reduced. Other energy dependences for the nucleon-nucleon cross sections have been also proposed.[17,18]

The average of $\omega^*_{\rm ij\to lm}$ over all possible values of the angle θ_{ij} between $\mathbf{p}_i$ and $\mathbf{p}_j$ leads to the decay rate $\omega^{*,\pi\nu}_{ij\to lm}$ to be inserted in the master equations. Since inequality (8) implies that if $p_l\le p_i$ or

$$p_j\le p_l\le(p_i^2+p_j^2)^{1/2}\ ,$$

then

$$-\frac{p_lp_m}{p_ip_j}\le\cos\theta_{ij}\le\frac{p_lp_m}{p_ip_j}\ , \tag{12a}$$

and if $p_i\le p_l\le p_j$, then

$$-1\le\cos\theta_{ij}\le 1\ , \tag{12b}$$

one obtains (in the case of proton-neutron interactions)

$$\omega^{*,\pi\nu}_{ij\to lm} = \tfrac{1}{2}\int_{\cos\theta_{ij,\min}}^{\cos\theta_{ij,\max}} \omega^{*,\pi\nu}_{ij\to lm}\, d\cos\theta_{ij}$$
$$= \frac{4KM\Delta\epsilon}{V(2p_ip_j)^{3/2}\sqrt{2B}}\left[\frac{1}{r+1}\right]\ln\left[\left[\frac{\sqrt{B+C}+\sqrt{2B}}{\sqrt{B+C}-\sqrt{2B}}\right]\Big/\left[\frac{\sqrt{B-C}+\sqrt{2B}}{\sqrt{B-C}-\sqrt{2B}}\right]\right], \tag{13}$$

where $\Delta\epsilon=\Delta\epsilon_l=\Delta\epsilon_m$, $B=(p_i^2+p_j^2)/2p_ip_j$, and $C=\cos\theta_{ij,\max}$, while

$$\omega^{*,\pi\pi(\nu\nu)}_{ij\to lm} = r\omega^{*,\pi\nu}_{ij\to lm}\ . \tag{14}$$

To avoid the singularity occurring when $\mathbf{p}_i=\mathbf{p}_j=\mathbf{p}_l=\mathbf{p}_m$, due to the inverse proportionality of the nucleon-nucleon cross section to the relative energy, it has been assumed that $\sigma_{ij}(E_{ij})=\sigma_{ij}(E_0)$ for $E_{ij}\le E_0$. $\omega^*_{ij\to lm}$ is the decay rate for the scattering of particles in definite states of the bins i and j to bins l and m and thus corresponds to $\omega_{ij\to lm}g_lg_m/\Delta\epsilon$ in the original formulation of HMB. Equations (1) thus reduce to

$$\frac{d(n_ig_i)^\pi}{dt} = \sum_{jlm}[\omega^{*,\pi\pi}_{lm\to ij}g_l^\pi n_l^\pi g_m^\pi n_m^\pi(1-n_i^\pi)(1-n_j^\pi)-\omega^{*,\pi\pi}_{ij\to lm}g_i^\pi n_i^\pi g_j^\pi n_j^\pi(1-n_l^\pi)(1-n_m^\pi)]$$
$$+\sum_{jlm}[\omega^{*,\pi\nu}_{lm\to ij}g_l^\pi n_l^\pi g_m^\nu n_m^\nu(1-n_i^\pi)(1-n_j^\nu)-\omega^{*\pi\nu}_{ij\to lm}g_i^\pi n_i^\pi g_j^\nu n_j^\nu(1-n_l^\pi)(1-n_m^\nu)]$$
$$-n_i^\pi g_i^\pi\omega^\pi_{i\to i'}g_{i'}^\pi\delta(\epsilon_i^\pi-\epsilon_F^\pi-B_i^\pi-\epsilon_{i'}^\pi)\ , \tag{15}$$

where the conservation of energy and momentum, in nucleon-nucleon scattering terms, has been already taken into account in the calculations of $\omega^*_{ij\to lm}$ and $\omega_{i\to i'}$ is yet given by (6).

In Fig. 2, for a nucleus with mass $A=185$, the crosses give the decay rates $\omega^*_{ij\to lm}$ for a given ϵ_i ($=97.5$ MeV) and different values of ϵ_j, as a function of ϵ_l. In the evaluation, nucleon-nucleon cross sections as given by (11a) and (11b) have been used, the bin width is 5 MeV, and the ordinate is given in units of τ_o^{-1} ($\tau_0=2.31\times10^{-23}$) as suggested by Harp *et al.*[11,12] The corresponding $\omega_{ij\to lm}g_lg_m/\Delta\epsilon$ of Harp *et al.*[11,12] (solid diamonds) are also reported for comparison.

The plateau in the $\omega^*_{ij\to lm}$ evaluated according to (13) corresponds to i, j, and l values satisfying conditions (12b). The increase of its ordinate as ϵ_j approaches ϵ_i, while ϵ_l is midway between their values, is due to the fact that in these conditions there is the possibility of scatter-

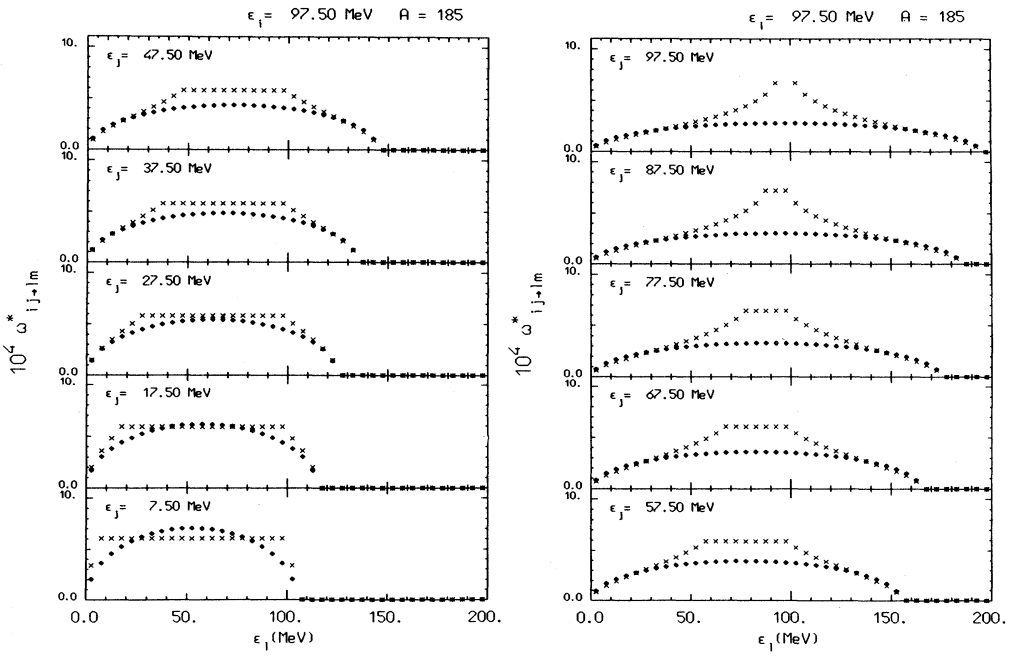

FIG. 2. Comparison of decay rates $\omega^*_{ij\to lm}$ (crosses) and $\omega_{ij\to lm}g_lg_m/\Delta\epsilon$ (solid diamonds), for given values of ϵ_i and ϵ_j, as a function of ϵ_l. These functions are defined only in correspondence to discrete values of ϵ_l. In the calculation displayed in the figure the bin width is 5 MeV. The unit of the ordinate is $1/\tau_o$, where $\tau_o=2.31\cdot10^{-23}$ is of the order of the time interval between two subsequent nucleon-nucleon collisions and its numerical value is that suggested by Harp, Miller, and Berne.[11] For $\epsilon_i=\epsilon_j=\epsilon_l=\epsilon_m=97.5$ MeV the calculated value of $\omega^*_{ij\to lm}$ is outside the range of values shown; in the units adopted it is equal to $0.126\ 10^{-1}$.

ing between pairs of nucleons with relative energies approaching zero, to which corresponds an increasingly greater cross section due to the inverse proportionality of σ_{ij} to the relative energy of interacting particles. The increase in the value of $\omega^*_{ij\to lm}$ occurring for $\epsilon_i=\epsilon_j=\epsilon_l=\epsilon_m$, is in fact due to the singularity already mentioned, and the corresponding numerical value of $\omega^*_{ij\to lm}$ is somewhat uncertain due to the arbitrary choice of the E_o value below which σ_{ij} is assumed to remain constant. The decrease of $\omega^*_{ij\to lm}$ toward the extremes of the allowed range of ϵ_l values is a consequence of the increasingly smaller interval of allowed $\cos\theta_{ij}$ values [condition (12a)].

It must be remarked that the differences between the decay rates evaluated by (13) and those based on Harp *et al.* approximation reduce greatly when one uses energy dependences for nucleon-nucleon cross sections different from (11a) and (11b), such as those suggested in Refs. (17 and 18). As in the case of $\omega_{ij\to lm}g_lg_m/\Delta\epsilon$ in HMB treatment, $\omega^*_{ij\to lm}$ is unchanged for exchange of i and j or l and m, while for the exchange of the pair ij with the pair lm:

$$\omega^*_{ij\to lm}=\omega^*_{lm\to ij}\left[\frac{p_lp_m}{p_ip_j}\right]. \tag{16}$$

III. INITIAL OCCUPATION NUMBER DISTRIBUTION

HMB master equations have been used by Blann[9] and Remington *et al.*[19] for evaluating the angle-integrated spectra of nucleons emitted in heavy ion reactions. These authors assumed that at $t=0$ the available entrance channel excitation energy is partioned only among the projectile nucleons, with each energy-conserving configuration bearing equal *a priori* weight. Assuming constant single-particle state densities, they thus obtain for the initial occupation number distribution $n_i(t=0)$ the following expression:

$$n_i(t=0)=\frac{n_o[(E-\epsilon_i+\Delta\epsilon/2)^{n_o-1}-(E-\epsilon_i-\Delta\epsilon/2)^{n_o-1}]}{E^{n_o-1}}, \tag{17}$$

where E is the excitation energy and n_o is equal to the mass number of the projectile, A_p.

This initial distribution, which does not consider the presence of holes and includes very excited particles, is basically different from that resulting from TDHF calculations or from the Fermi jet distribution (FJD) calculated by coupling translational and internal momenta.

As the two fragments approach one another, to form a composite system, the FJD, which represents the momentum distribution before reactions take place, is modified by the action of the mean field acting between the two fragments and by the effect of the nucleon-nucleon collisions. We assume that the mean field has a minor effect in modifying the momentum distribution of single particles, and we account for the nucleon-nucleon interactions by means of the HMB master equations starting with the FJD for $t=0$.

The calculation of the number of states of the composite system, $N_i=n_ig_i$, occupied in each bin by the projectile and the target nucleons, in the case of a FJD, is straightforward. The essential quantities entering the calculation are (i) the translational momentum of a given nucleon in the two ion center-of-mass system, equal to

$$p_t^p=\left[\frac{2E_{\rm inc}}{A_p}\right]^{1/2}\left[\frac{A_T}{A_p+A_T}\right] \tag{18a}$$

for the projectile nucleons ($E_{\rm inc}$ is the projectile energy in the lab system and A_p and A_T the mass numbers of, respectively, the projectile and the target) and to

$$p_t^T=\left[\frac{2E_{\rm inc}}{A_p}\right]^{1/2}\left[\frac{A_p}{A_p+A_T}\right] \tag{18b}$$

for the target nucleons, and (ii) the Fermi momentum p_F.

With reference to Fig. 3(a), to each nucleon momentum $\mathbf{p}$ we associate a density of occupied states $\rho(\mathbf{p})$ that is equal to the Fermi density of the projectile when the end point of $\mathbf{p}$ falls within the region $\mathcal{P}$, equal to the Fermi density of the target when it falls within the region $\mathcal{T}$, equal to the sum of the two when it falls in the region where the two Fermi spheres superimpose, and zero otherwise. By a transformation to the variables ϵ and θ, ($\epsilon=|\mathbf{p}|^2/2M$ and θ is the angle between $\mathbf{p}$ and the direction of the translational momenta $\mathbf{p}_t^P$ and $\mathbf{p}_t^T$) one obtains a density of occupied states $N(\epsilon,\theta)$:

$$N(\epsilon,\theta)d\epsilon\,d\theta=2\pi\rho(\mathbf{p})p^2dp\,\sin\theta\,d\theta\,, \tag{19}$$

and, finally, the number of occupied states within each bin, is obtained by integration

$$N_i=\int_{\epsilon_i-\Delta\epsilon/2}^{\epsilon_i+\Delta\epsilon/2}d\epsilon\int_0^{\pi}N(\epsilon,\theta)d\theta\,. \tag{20}$$

The occupation numbers are $n_i=N_i/g_i$, where g_i, referring to the composite system, are given by (3) [(with $Z=Z_p+Z_T$ or $N=N_p+N_T$)].

The values of $n_i(t=0)$ calculated for neutrons in the case of (a) 600 MeV [20] Ne ions incident upon [165]Ho, and

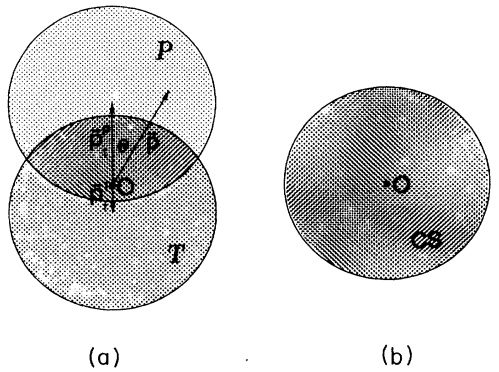

FIG. 3. (a) Momentum-space representation of the Fermi spheres for projectile ($\mathcal{P}$) and target ($\mathcal{T}$) nucleons. The centres of the two spheres are displaced from the centre O of the sphere corresponding to the composite system, by, respectively, p_t^p and p_t^T; (b) Fermi sphere for the composite system (in the ground state).

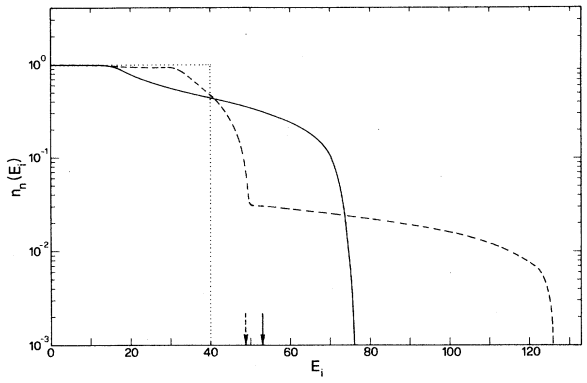

FIG. 4. Occupation number distribution of neutron states of the composite nucleus, at the beginning of the deexcitation cascade, in the case of 600 MeV ^{20}Ne ions on ^{165}Ho (dashed line) and 800 MeV ^{40}Ar on ^{40}Ca (full line). Neutrons with energy in excess of, respectively, the dashed and the full arrow are in the continuum. The dotted line gives the occupation number distribution for a zero temperature Fermi gas.

(b) 800 MeV ^{40}Ar ions on ^{40}Ca, are shown in Fig. 4. The calculations are made using a value of 40 MeV for the Fermi energy of projectile, target and composite nucleus, assuming a central collision and also that the Coulomb potential energy of the two ions is converted back into translational kinetic energy as they fuse. The hypothesis of purely central collisions, to describe fusion and quasifusion processes is common to other theoretical approaches like the ones discussed by Iwamoto[8] and Blann,[9] but is different from that made in other works (see, for instance, Randrup and Vandenbosch[17] and Leray *et al.*[20]) where a dynamical theory of the fusion process is developed to evaluate the trajectories of the colliding ions; however, in the case we will consider, the deflection of the fusing ions, in a purely Coulomb field, before their volumes start to overlap, is at most a few degrees.

Figures 3(a) and 3(b) (which refers to the composite nucleus in its ground state) and Fig. 4 show that the initial occupation number distribution, evaluated in this way, is characterized by the presence of excited particles and an equal number of holes with respect to the ground-state distribution. The presence of deep hole states thus makes it possible, contrary to what happens in processes induced by a light particle, for a highly excited particle to gain energy by scattering the collision partner to a hole state, and thus, in the early states of the intranucleon collision cascade, the time-dependent occupation number distribution may contain particles more energetic than those contained in the initial distribution with a consequent hardening of the emitted particle spectrum.

IV. COMPARISON OF THEORETICAL PREDICTIONS WITH THE EXPERIMENTAL DATA

The theory outlined in Secs. II and III has been used to analyze the neutron multiplicity distributions measured in coincidence with an evaporation residue by Holub *et al.*[21,22] and Hilscher *et al.*[23], in reactions induced on ^{165}Ho by ^{20}Ne and ^{12}C ions with energy varying from 20 to 30 MeV/nucleon, and by Rösch *et al.*[24] (see also Lassen[25]), in the case of reactions induced by 20 MeV/nucleon ^{40}Ar ions on ^{40}Ca. These spectra are similar in appearance to those of neutrons emitted in reactions induced by light projectiles and the low energy evaporative component may easily be separated from the harder component due to preequilibrium emissions.

In the case of reactions induced by ^{12}C and ^{20}Ne the experimental multiplicity distributions in the center-of-mass (c.m.) system have been obtained from the double differential multiplicities, measured in the lab system, by fitting the hardest parts of each of them with the function

$$M(E,\theta)=A(\theta)Ee^{-E/T(\theta)} \tag{21}$$

and then transforming to the c.m. system of the two colliding ions, using for $A(\theta)$ and $T(\theta)$, at unmeasured angles, values obtained by linear interpolation. We did not extrapolate the measured distributions to energies greater than 85 MeV, where most of the measured distributions stop. After transformation to the c.m. system, an integration over the emission angle is made to obtain the angle integrated multiplicity distributions.

In the case of the reactions induced by ^{40}Ar ions on ^{40}Ca, the c.m. multiplicity distribution was taken from Lassen.[25]

The experimental data are compared with the theoretical predictions obtained solving the master equations (15) with the initial conditions outlined in the preceding Section. In all calculations, a value of 40 MeV was used for the Fermi energy of the projectile, target and composite nucleus, and in evaluating the decay rates for emission of particles into the continuum, semiclassical expressions have been used for simplicity for the inverse neutron and proton cross sections:

$$\sigma_{\rm inv}(\epsilon_n)=\pi R_{on}^2 C_n A^{2/3}\left[1+\frac{\beta}{\epsilon_n}\right], \tag{22}$$

with C_n and β as given by Dostrovsky *et al.*[26] and

$$\sigma_{\rm inv}(\epsilon_p)=\pi R_{op}^2 A^{2/3} C_p\left[1-\frac{C_b}{\epsilon_p}\right], \tag{23}$$

where C_b is the proton Coulomb barrier. The values chosen for R_{on} and $R_{op}^2 C_p$ were, in each case, those that reproduced correctly the values of the inverse cross sections calculated by the optical model at an energy of about 20–30 MeV.[27,28]

The coefficient K appearing in 11(a) and 11(b) was the only free parameter in the calculations. For it, values of 500, 250, and 125 fm^2·MeV were used corresponding respectively to free nucleon-nucleon cross sections and cross sections scaled by factors 2 and 4 with respect to the free cross section values. In all calculations the energy E_o below which the nucleon-nucleon cross section is assumed to be constant was taken to be 1.25 MeV and for r the value $r=0.333$ was assumed.

The system of differential equations (15) was integrated by the method of Kutta-Merson that represents a modification of the fourth order Runge-Kutta procedure and provides a technique for automatic interval adjustment.[29] The energy bin interval was in all cases 4 MeV.

In all cases considered the accretion of the hardest part of nucleon spectra was found to be complete after a time $T \approx 10^{-22}$ sec since the beginning of nucleon-nucleon interactions, while the emitted nucleon yield in the lowest energy region (corresponding to $\epsilon_n \leq 35$ MeV) was found to increase up to the longest times we considered, $\approx 2 \times 10^{-21}$ sec.

In Fig. 5 the comparison between the experimental and calculated neutron multiplicities are shown for the very asymmetric systems C+Ho and Ne+Ho. In all cases the master equations were integrated up to $T = 5 \cdot 10^{-22}$ sec and folded with a Gaussian resolution function having a FWHM equal to the energy resolution of the experimental distributions.

The dotted, dashed, and full lines correspond to the use of nucleon-nucleon cross sections equal to, respectively, the free values and values scaled by factors 2 and 4. The comparison is on an absolute scale. The spectrum calculated using a scaling factor 4 closely resembles that obtained by means of a generalization of the exciton model recently discussed[30] which consists in neglecting the hole excitations and in considering simply the excited particles that, in the case of very asymmetric systems, like those here considered, are essentially the projectile nucleons. This strict correspondence demonstrates that for asymmetric systems like those here considered (asymmetry parameter $y = A_p / A_T \leq 0.13$) the effect of interaction between excited nucleons in the presence of deep holes is of negligible importance. Indeed, a hardening of the nucleon spectrum due to nucleon-nucleon interactions occurs, as shown in Fig. 6, where, in the case of the interaction of 600 MeV ^{20}Ne ions on ^{165}Ho, the energy distributions of neutrons resulting from the translational and internal momentum coupling (full line histogram) is compared with the emitted neutron multiplicity distribution evaluated at a time $T = 5 \times 10^{-22}$ sec (dashed line histogram). One finds neutrons with energy in excess of the kinematical limit $[E_K = (p_t^p + p_F)^2 / 2m_n - (\epsilon_F + B) \approx 80$ MeV], but their yield is so small that they are barely detectable. However, one should remark that in the case of very asymmetric systems the interactions leading to the highest energy nucleons involve two projectile nucleons moving in the forward direction. One should expect, for these collisions, decay rates larger than those evaluated assuming completely random directions of colliding nucleons, as in (13). This would be a consequence of the use of interaction cross sections inversely proportional to the relative energy and to the reduction in the available final phase space. Thus, a more approximate calculation (which would involve the evaluation of the time dependent momentum distribution instead of the energy distribution only) would presumably lead, in the case of asymmetric systems, to spectra harder than those reported here.

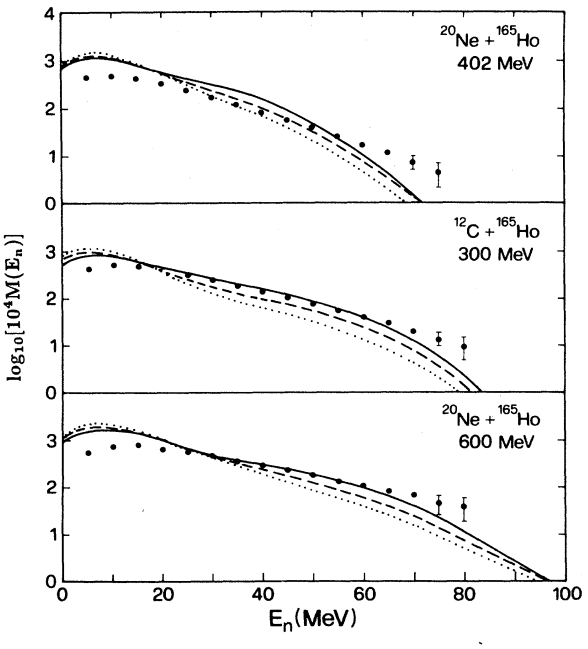

FIG. 5. Angle integrated c.m. multiplicity distributions of preequilibrium neutrons for the reactions indicated. The experimental results are given by the full dots, the theoretical expectations by the dotted, dashed and full lines. See the text for further details.

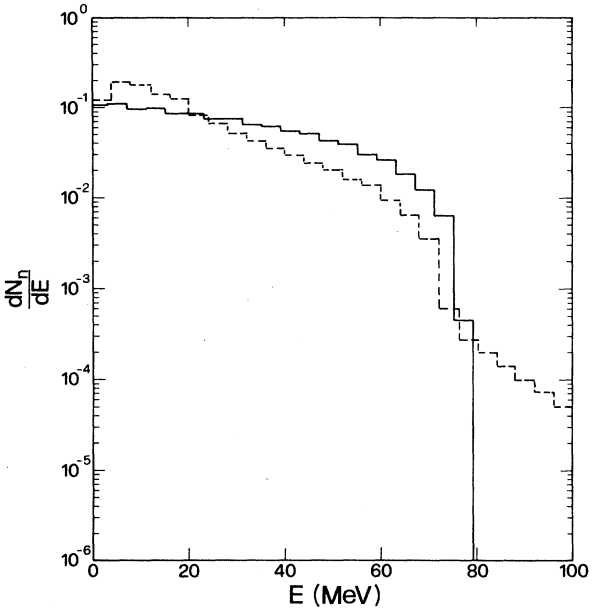

FIG. 6. Comparison, in the case of the interaction of 600 MeV ^{20}Ne ions with ^{165}Ho, of the energy distribution of neutrons resulting from the translational and internal momentum coupling (full line histogram) with the emitted neutron multiplicity distribution evaluated at a time $T = 5 \times 10^{-22}$ sec (dashed line hystogram). This distribution extends also beyond 100 MeV, decreasing exponentially.

Basically different is the result we find when we consider a symmetric system ($y = 1$) such as ^{40}Ar+^{40}Ca at 800 MeV. In this case, the maximum neutron energy at the beginning of the nucleon-nucleon interaction cascade, corresponding to the kinematical limit, is only ≈ 20.3 MeV, an energy considerably smaller than that to which the experimental neutron spectrum extends. Also considering the smearing due to the low-energy resolution affecting these data, one cannot bring the calculations in

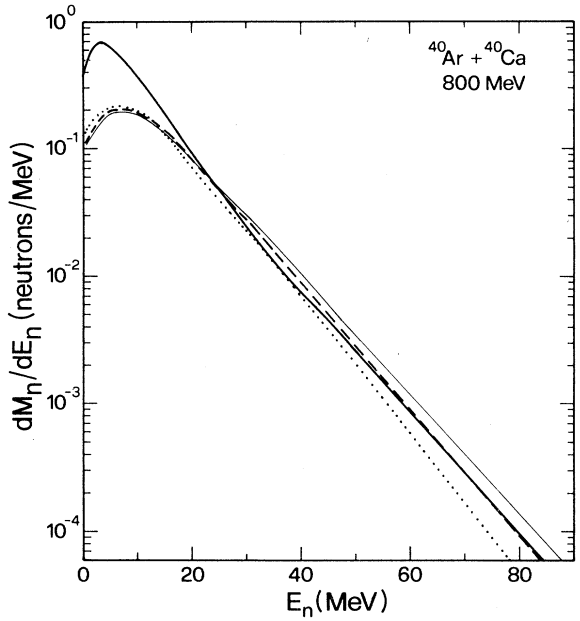

FIG. 7. Comparison of the neutron spectrum from the interaction of 800 MeV ^{40}Ar ions with ^{40}Ca (Ref. 25) (thick full line) with the spectra calculated using free nucleon-nucleon cross sections (thin full line) and cross sections scaled, respectively, by a factor 2 (dashed line) and 4 (dotted line).

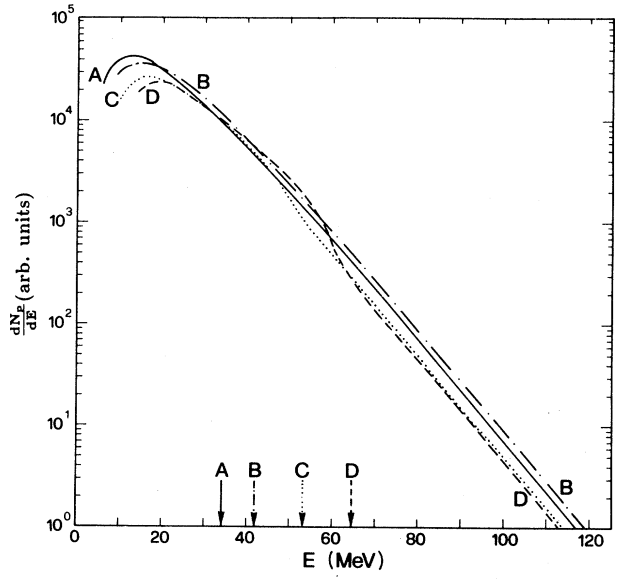

FIG. 8. Calculated proton spectra ($T \approx 2\times10^{-22}$ sec) following the interaction of (A)^{32}S and ^{27}Al ($y=0.84$), (B)^{32}S and ^{58}Ni ($y=.55$), (C)^{32}S and ^{120}Sn ($y=0.27$), (D)^{32}S, and ^{197}Au ($y=0.16$). The energy of the incident ^{32}S ion beam is, in all cases, equal to 679 MeV, and free nucleon-nucleon cross sections have been used in the calculation. The arrows indicate, in each case, the highest possible energy of protons at the beginning of the interaction cascade resulting from the kinematical coupling of the translational and internal momentum of either the projectile or the target.

agreement with the data in the absence of a considerable hardening of the spectrum due to subsequent nucleon collisions. The comparison in Fig. 7 of the experimental neutron spectrum, reported by Lassen,[25] (thick full line) with the ones calculated using free nucleon-nucleon cross sections (thin full line) and cross sections scaled, respectively, by a factor 2 (dashed line) and 4 (dotted line) shows that this hardening occurs. In all cases the master equations have been integrated up to $T=12\cdot10^{-22}$ sec. As in previous cases the comparison is on an absolute scale without any normalization and the calculated spectra have been smeared using a Gaussian resolution function. The calculated spectra are in excellent agreement with the measured spectrum thus showing that nucleon-nucleon interactions have considerably hardened the neutron energy distribution at the beginning of the nucleon-nucleon interaction cascade.

The importance of nucleon-nucleon interactions is also indicated by the dependence of the calculated neutron yield on the scaling factor multiplying the free nucleon-nucleon cross section. In this case a larger nucleon-nucleon cross section results in an increased yield of high-energy neutrons. An increase of the interaction cross section increases the probability of producing high energy nucleons in nucleon-nucleon interactions. At the same time, the probability of their emission into the continuum decreases. The emitted nucleon yield depends on both these two opposite tendencies and the observed increase in the yield of the emitted neutrons for a larger nucleon-nucleon cross section demonstrates that the first effect is predominant.

In the case of the very asymmetric systems previously considered the amount of high-energy nucleons at the beginning of the interaction cascade was too small to produce any significant yield of high-energy nucleons as a result of the nucleon-nucleon interactions and, in practice, the second effect is the only one operating. Thus, an increase of the nucleon-nucleon cross section reduced the yield of the high-energy neutrons.

In Fig. 8 are shown, for systems of different symmetry [(A)^{32}S+^{27}Al ($y=.84$, full line), (B)^{32}S+^{58}Ni ($y=.55$, dotted and dashed line), (C)^{32}S+^{120}Sn($y=.27$, dotted line), (D) ^{32}S+^{197}Au ($y=.16$, dashed line)], the calculated spectra of preequilibrium protons at a time $\approx2\times10^{-22}$ sec. The energy of the incident ^{32}S ion beam is in all cases equal to 679 MeV and, in the calculation, free nucleon-nucleon cross sections have been used. The arrows indicate, in each case, the highest energy of the protons at the beginning of the interaction cascade resulting from the kinematical coupling of the translational and internal momentum. The importance of the nucleon-nucleon interaction is shown by the fact that, in spite of the considerably different initial energy distributions the emitted particle spectra are very similar and, if there is a difference, the softest spectrum corresponds to the hardest initial distribution. In case (D) one may identify two components of the calculated spectrum, one corresponding to the particles emitted immediately, without any interaction, that ends at the energy corresponding to

the arrow (D), and one of protons that acquired energy in at least one previous nucleon-nucleon interaction. The two contributions are barely observable in the case of ^{120}Sn, and cannot be separated in all the other cases.

The hardening of the nucleon spectrum obviously depends on the probability of interaction of two particles of sufficient initial energy which is proportional to the product of the corresponding number of occupied states $n_i g_i n_j g_j$ and the number of available deep holes where one of the two particles may scatter, which is proportional to $(1-n_l)g_l$. The comparison, in Fig. 4, of the initial occupation number distributions corresponding to Ne+Ho and Ar+Ca shows that the probability of a nucleon-nucleon interaction producing nucleons with energy greater than that of the interacting nucleons may be orders of magnitudes greater in the symmetric case.

All the calculations discussed in this section have been also repeated using the nucleon-nucleon cross section suggested by Cassing.[18] In all the cases the results were found to differ very slightly, from a quantitative point of view, from those obtained by using the free nucleon-nucleon cross sections.

V. CONCLUSIONS

The calculations presented in this work suggest that the nucleon-nucleon interactions may lead to a considerable hardening of the primary nucleon spectrum when the asymmetry parameter $y \geq 0.13$. To obtain this result, one must explicitly consider the possibility of interactions between unbound nucleons in the presence of deep holes. This may be done in the most natural way by means of the HMB master equation approach.

The spectrum of emitted neutrons, in the case of the symmetric system ^{40}Ar+^{40}Ca, is an excellent agreement with the experimental one[25] though the neutrons initiating the equilibration cascade have a much softer initial energy distribution.

In case of very asymmetric systems, like ^{12}C+^{165}Ho or ^{20}Ne+^{165}Ho, the density of occupied continuum states at the beginning of the interaction cascade is too small to allow the nucleon-nucleon interactions to produce a noticeable effect. In this case the absolute multiplicity is correctly reproduced but the neutron spectra appear too soft. This may be an indication that higher-order momentum components in the primary spectrum should be considered. As mentioned in Sec. I, the semiclassical procedure we adopt to evaluate the primary nucleon energy distribution is only a first-order approximation and a more realistic quantum-mechanical approach should be used as suggested by Cassing.[5,7] The result we obtain seems, however, to imply that the primary nucleon energy distribution we use is not dramatically softer than that necessary to obtain a satisfactory reproduction of the data in the case of very asymmetric systems.

We did not make a best fit parameter search; in fact the only parameter we varied was the factor scaling the free nucleon-nucleon cross sections and the results we obtain (even taking into account the dependence of this conclusion on the set of parameters we adopt) seem to indicate that the nucleon-nucleon cross-section should be somewhat reduced with respect to the free ones. However, any definite conclusion concerning this point should be deferred to a more extensive analysis of the experimental data than that here presented.

ACKNOWLEDGMENTS

It is a great pleasure to thank P. E. Hodgson for a careful reading of the manuscript and enlightening suggestions. The work has been partly supported by the Italian Ministry of Public Instruction.

[1] J. Negele, Rev. Mod. Phys. **54**, 913 (1982).
[2] W. Cassing, Z. Phys. A **326**, 21 (1987).
[3] J. Aichelin and G. Bertsch, Phys. Rev. C **31**, 1730 (1985).
[4] H. Kruse, B. V. Jacak, J. J. Molitoris, G. D. Westfall, and H. Stöcker, Phys. Rev. C **31**, 1770 (1985).
[5] W. Cassing, Z. Phys. A **327**, 87 (1987).
[6] W. Cassing, Z. Phys. A **327**, 447 (1987).
[7] W. Cassing, Z. Phys. A **329**, 471 (1988).
[8] A. Iwamoto, Phys. Rev. C **35**, 984 (1987).
[9] M. Blann, Phys. Rev. C **23**, 205 (1981); **31**, 1245 (1985); **35**, 1581 (1987).
[10] C. J. Bishop, I. Halpern, R. W. Shaw, Jr., and R. Vandenbosch, Nucl. Phys. **A198**, 161 (1972).
[11] G. D. Harp, J. M. Miller, and B. J. Berne, Phys. Rev. **165**, 1166 (1968).
[12] G. D. Harp and J. M. Miller, Phys. Rev. C **31**, 847 (1971).
[13] J. B. Bondorf, J. N. De, G. Fai, A. O. T. Karvinen, B. Jakobsson, and J. Randrup, Nucl. Phys. **A333**, 285 (1980).
[14] M. C. Robel, Lawrence Berkeley Laboratory Report LBL-8181, 1979 (unpublished).
[15] J. Aichelin, J. Phys. (Paris) Colloq. **47**, C4-63 (1986).
[16] K. Kikuchi and M. Kawai, *Nuclear Matter and Nuclear Reactions* (North-Holland, Amsterdam, 1968).
[17] J. Randrup and R. Vandenbosch, Nucl. Phys. **A474**, 219 (1987).
[18] W. Cassing, K. Niita, and S. J. Wang, Z. Phys. A **331**, 439 (1988).
[19] B. A. Remington, M. Blann, A. Galonsky, L. Heilbronn, F. Deak, A. Kiss, and Z. Seres, Phys. Rev. C **38**, 1746 (1988).
[20] S. Leray, G. La Rana, C. Ngo, M. Barranco, M. Pi, and X. Vinas, Z. Phys. A **320**, 383 (1985).
[21] E. Holub, D. Hilscher, G. Ingold, U. Jahnke, H. Orf, and H. Rossner, Phys. Rev. C **28**, 252 (1983).
[22] E. Holub, D. Hilscher, G. Ingold, U. Jahnke, H. Orf, H. Rossner, W. P. Zank, W. W. Schröder, H. Gemmeke, K. Keller, L. Lassen, and W. Lücking, Phys. Rev. C **33**, 143 (1986).
[23] D. Hilscher, H. Rossner, A. Gamp, U. Jahnke, B. Cheynis, B. Chambon, D. Drain, C. Pastor, A. Giorni, C. Morand, A. Dauchy, P. Stassi, and G. Petitt, Phys. Rev. C **36**, 208 (1987).
[24] W. Rösch, A. Richter, G. Schrieder, R. Gentner, K. Keller, L. Lassen, W. Lücking, R. Schreck, W. Cassing, and H. Gemmeke, Phys. Lett. B **197**, 19 (1987).
[25] L. Lassen, *Proceedings of the 5th International Conference on Nuclear Reaction Mechanisms, Varenna, 1988,* edited by E. Gadioli (Ricerca Scientifica ed Educazione Permanente, Milano, 1988), Suppl. 66.

[26]I. Dostrovsky, Z. Fraenkel, and G. Friedlander, Phys. Rev. **116**, 683 (1959).
[27]A. Linder, Institut für Kernpkysik, Frankfurt, Report IKF-17, 1966.
[28]G. S. Mani, M. A. Melkanoff, and I. Iori, Centre d'Etudes Nucleaires de Saclay, Report 2379, 1963.
[29]L. Fox, *Numerical Solutions of Ordinary and Partial Differential Equations,* (Addison-Wesley, London, 1962).
[30]E. Fabrici, E. Gadioli, and E. Gadioli Erba, Phys. Rev. C **40**, 459 (1989).